Available online at www.sciencedirect.com

ScienceDirect

Ceramics International 40 (2014) 1329–1334

CERAMICS INTERNATIONAL

www.elsevier.com/locate/ceramint

Fabrication and properties of SiC/mullite composite porous ceramics

Yani Jing[a], Xiangyun Deng[a,b,*], Jianbao Li[a,c], Chengying Bai[a], Wenkai Jiang[a]

[a]Key Laboratory of Ministry of Education for Advanced Materials in Tropical Island Resources, Hainan University, Haikou 570228, China
[b]College of Physics and Electronic Information, Tianjin Normal University, Tianjin 300387, China
[c]State Key Laboratory of New Ceramics & Fine Processing, Department of Materials Science and Engineering, Tsinghua University, Beijing 100084, China

Received 20 May 2013; received in revised form 4 June 2013; accepted 2 July 2013
Available online 8 July 2013

Abstract

SiC/mullite composite porous ceramics were prepared from a mixture of calcined kaolin, aluminum hydroxide, silicon carbide, and graphite. The above mixture was heated in air at 1250–1450 °C to produce pores by burning graphite and bond the SiC particles by reaction-derived mullite. The reaction bonding behavior, open porosity, firing shrinkage, and mechanical strength of the composites were investigated as a function of the mass ratio of calcined kaolin and $Al(OH)_3$, sintering temperature, holding time, and graphite content. In addition, the phase composition and microstructure of the composites were also studied. The results show that when the mass ratio of calcined kaolin:$Al(OH)_3$ is 1:1.5, in the absence of graphite, the flexural strength and the open porosity of the composites were 48.14 MPa and 33.97%, respectively. However, when 15% graphite was added to the above composition, a flexural strength of 27.26 MPa was achieved at an open porosity of 48.80%.

Keywords: D. Mullite; Porous ceramics; SiC

1. Introduction

Porous ceramics have been widely used in many areas, such as filters, membranes, catalyst supports, heat exchangers, electrodes sensors, and so on [1–4]. Recently, due to their low thermal expansion coefficient, high thermal conductivity and excellent mechanical properties [5–7], porous SiC ceramics attract more and more attention from material researchers. However, it is hard to sinter SiC ceramics at moderate temperatures due to the covalent nature [8,9]. One effective way of fabricating porous SiC ceramics at low temperatures is to add a small amount of bonding phases to bond SiC particles together. She and co-workers [10,11] have reported an oxidation bonding technique for the preparation of SiC porous ceramics at low temperatures. In order to realize the low-temperature fabrication of porous SiC ceramics, some clay (such as kaoline) can be added to bond SiC. It is necessary to choose a suitable interparticle phase between SiC particles while maintaining the good properties of SiC porous ceramics in order to reduce the processing cost.

Mullite ($3Al_2O_3 \cdot 2SiO_2$) has a close thermal expansion match and good chemical compatibility with SiC ensures mullite bonded porous SiC ceramics with the excellent high-temperature strength and thermal shock resistance [12]. Kaolin was well studied in the past decades for serving the conventional ceramics and there have been renewed interests in the conversion of kaolin to mullite owing to its low cost and relatively low sintering temperature [13–17]. A big problem, however, is that the mullite made by the conventional method is generally dense due to the excess SiO_2 existing in kaolin. The addition of Al_2O_3 powders can reduce the amount of glass phase (SiO_2) and increase the amount of mullite [18,19].

In the present work, calcined kaolin and aluminum hydroxide as alumina sources were used as starting materials for mullite, which then bonded SiC particles to form a composite at relatively low temperatures. Graphite powder was used as the pore former. The sintering behaviors, porosity, firing shrinkage and mechanical strength of the SiC/mullite composite porous ceramics were investigated.

*Corresponding author. Tel./fax: +86 898 66252327.
E-mail addresses: xiangyundtj@126.com, jiangwenkai555@126.com (X. Deng).

0272-8842/$ - see front matter © 2013 Published by Elsevier Ltd and Techna Group S.r.l.
http://dx.doi.org/10.1016/j.ceramint.2013.07.013

2. Experimental procedure

The raw materials used in our experiment are commercially available SiC powder, calcined kaolin and aluminum hydroxide. Their mean particle sizes (D50) are 23.0, 2.6, 11.7 μm, respectively. The graphite (18.7 μm) powders were employed as the pore-former to fabricate porous SiC/mullite ceramics with different porosity. SiC, kaolin, aluminum hydroxide and graphite were mixed at different mass ratios and ball-milled in ethanol for 24 h at a rotation speed of 100 rpm to obtain homogeneous slurries. After being dried at 80 °C in an oven, mixed with certain binder (CMC) in a mortar and sieved through a 100-mesh screen, the mixed powders were uniaxially pressed into the specimens under 24 MPa using a steel die. Compositions of the specimens used in this study are listed in Table 1. The specimens were heated to burn out graphite before 850 °C at a heating rate of 2 °C/min and then at 1250–1450 °C for different soaking time with a heating rate of 5 °C/min.

The composite powders were examined by thermogravimetry analysis and differential scanning calorimetry analysis (TG–DSC STA449C, Netzsch Co. Ltd. Germany) at a heating speed of 10 °C/min in flowing air. The open porosity and bulk density were determined by the Achimedes method with distilled water as the liquid medium. Specimens were machined to the dimension of 3.0 mm × 4.0 mm × 36.0 mm to test the flexural strength via the three-point bending test (Model AGS-X,Shimadzu, Japan) with a support distance of 30.0 mm and a cross-head speed of 0.5 mm/min. The strength was obtained by the average value for five samples Phase analysis was conducted by X-ray diffraction (XRD), via a computer-controlled diffractometer (D8 Advance, Brucker, Germany) with Cu Kα radiation (wavelength of 0.154178 nm). Microstructure and morphology of porous SiC ceramics were observed by a field emission scanning electron microscope (FESEM, Hitachi S-4800, Japan).

3. Results and discussion

3.1. Reaction bonding behavior

Fig. 1 shows the TG–DSC curves of the green powder with graphite. An endothermic DSC peak was observed at ~280 °C accompanied with a distinct weight loss, which was attributed to the formation of alumina due to decomposition of aluminum hydroxide. It is known that C oxidation begins at ~600 °C and completes at ~900 °C, while SiC starts to oxidize to SiO_2 at ~750 °C[20]. This can be observed from the exothermic peak at 785.1 °C accompanied with a mass loss in the TG curve, up to 14.55 wt%, in the temperature range 600–900 °C. Thus, heating rate must be kept slow between 600 °C and 900 °C, because a high heating rate may result in the vast release of CO_2 owing to burning of graphite, leading to the collapse of green bodies. The endothermal peak at 983.7 °C corresponds to the formation of Al–Si spinel ($SiAl_2O_4$), γ-Al_2O_3 and amorphous silica [21,22]. Moreover, another endothermic peak was observed at ~1390.8 °C, which may be due to the mullitization of SiO_2 and Al_2O_3. Fig. 2 shows the XRD patterns of porous SiC ceramics sintered at different temperatures for 3 h. SiC, cristobalite, and Al_2O_3 exist at all the five sintering temperatures, weak mullite peaks appeared at 1250 °C, and no other new phase has formed upon 1250 °C. The peak intensity of mullite did not change as temperature increased from 1250 to 1350 °C. When the sintering temperature was increased to 1400 °C, the mullite peaks are obvious, so it can be inferred that the endothermic peaks near 1400 °C. At 1400–1450 °C, the amount of Al_2O_3 decreased abruptly as extensive mullitization occurred. Also, the glass phase was consumed rapidly with the formation of secondary mullite at 1350–1450 °C. In summary, the excess SiO_2 in calcined kaolin (metakaolin) can be consumed by adding alumina and increase the amount of mullite, which is beneficial for obtaining SiC/mullite ceramic composites. This can be explained by the following reactions [23]:

$$3(Al_2O_3 \cdot 2SiO_2)(metakaolin) \overset{>1050\ ^\circ C}{\Longrightarrow} (3Al_2O_3 \cdot 2SiO_2)(mullite) + 4SiO_2 \quad (1)$$

$$3Al_2O_3 + 2SiO_2 \overset{>1300\ ^\circ C}{\Longrightarrow} (3Al_2O_3 \cdot 2SiO_2)(\text{mullite}) \quad (2)$$

Table 1
Compositions of the green bodies used in this study.

Mixture	$\frac{SiC}{SiC+Al(OH)_3+Kaolin(wt\%)}$	Kaolin:Al(OH)$_3$ (wt%)	$\frac{Graphite}{SiC+Kaolin+Al(OH)_3(wt\%)}$
1	60	30:70	0
2	60	35:65	0
3	60	40:60	0
4	60	45:55	0
5	60	40:60	10
6	60	40:60	15
7	60	40:60	20
8	60	40:60	25

3.2. Microstructural evolution

Fig. 3 shows the SEM micrograph of the specimen sintered in air at 1400 °C for 3 h. It exhibits a stable structure with

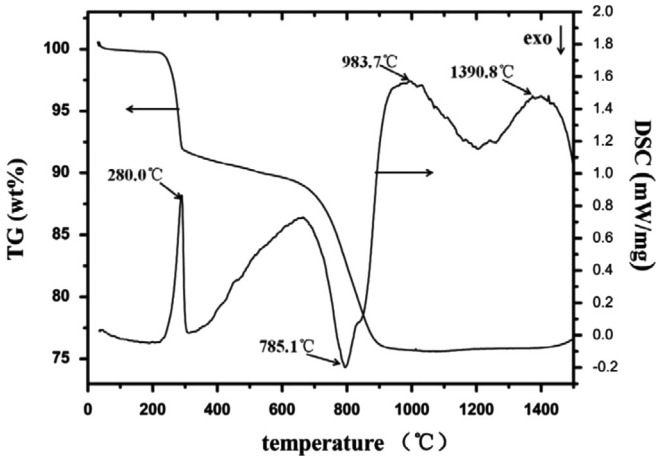

Fig. 1. TG–DSC curves of the dried starting powder mixture with graphite at a heating rate of 10 °C/min in air. (For interpretation of the references to color in this figure, the reader is referred to the web version of this article.)

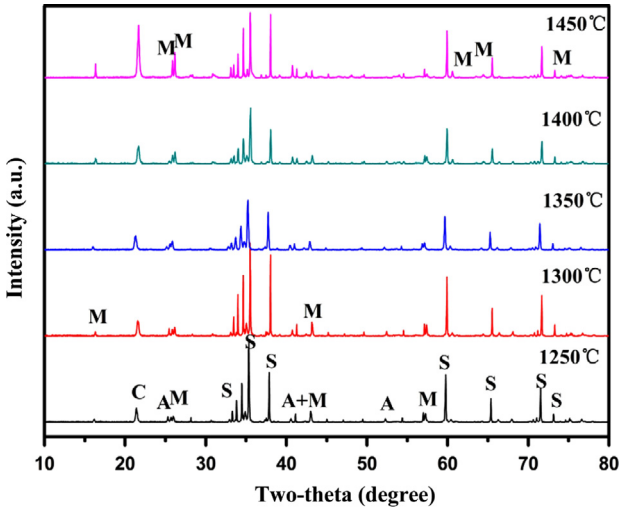

Fig. 2. XRD patterns of the specimens with the mass ratio of kaolin and Al $(OH)_3$ in green bodies was 40:60, sintered at indicated temperature for 3 h in air. (S is SiC, M is mullite, C is cristobalite and A is Al_2O_3). (For interpretation of the references to color in this figure legend, the reader is referred to the web version of this article.)

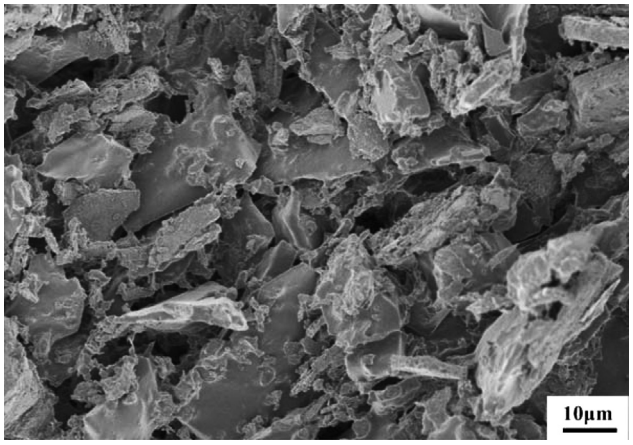

Fig. 3. SEM micrograph of the specimen sintered at 1400 °C for 3 h in air.

distinct connected pores, and well-developed necks are observed between the SiC particles. The pores are mainly generated by both stacking of SiC particles and burning of graphite. At the same time, small number of floccules were observed on the surface of SiC particles. It can be deduced according to the results of the above XRD patterns that these floccules mainly consisted of amorphous silica and unreacted alumina. Fig. 4 shows the detailed structure of the pores in the specimen sintered in air at 1400 °C for 3 h. Well-developed necks were formed between the SiC particles. In addition, mullite was observed not only on the neck of porous ceramics, but also on the surface of SiC (Fig. 4a, marked by arrows). The porous structure is considered to be stabilized by cristobalization and mullitization rather than the coarsening of SiC grains. As shown in Fig. 4b, the type of pores is attributed to further oxidation of SiC particles during the sintering process. Although oxygen can diffuse into the outer of SiC particles, gaseous oxidation products (SiO, CO) are trapped in the oxidation-derived silica layer and cause the formation of bubbles [24].

3.3. Porosity and mechanical strength

Fig. 5 shows plots of the flexural strength and open porosity of the composites as the functions of sintering temperature and soaking time, where 15% graphite was used as the pore-forming agent. The flexural strength increased slightly as the sintering temperature was raised from 1250 to 1350 °C; however, it increased significantly with further increase in sintering temperature to 1450 °C. It can be confirmed from Fig. 2, the amount of Al_2O_3 decreased abruptly leading to more extensive mullitization, and distinct cristobalite peaks appeared at 1350–1450 °C. Mullite and cristobalite can enhance the bonding between SiC particles and improve the strength of porous SiC ceramics [25,26], while the open porosity decreases continuously with increasing sintering temperature from 1250 to 1450 °C. An increase in the flexural strength was achieved by extending the soaking time from 1 to 5 h at 1400 °C, whereas a rapid decrease in open porosity was observed as the soaking time was increased from 3 to 5 h.

All the samples exhibited small variations in dimension (a 1inear expansion of 0.08–0.16%) after the sintering process. Almost no change in the particle morphologies were observed after the sintering process, as shown in Fig. 3. Further, necks between SiC particles were formed during the sintering process through reaction bonding. Therefore, rearrangements in SiC particles could not take place. Fig. 6 displays that the linear expansion of sample first increased and then decreased with the increase of the sintering temperature. The densification behavior was mainly related to the dehydration of $Al(OH)_3$, mullite formation, and the liquid phase which mainly derived from SiO_2 and Al_2O_3 at higher temperatures. When the sintering temperature was increased from 1350 to1450 °C, the relative contents of mullite and cristobalite increased in the sample, and it could be inferred that much more liquid was present in the sample based on the above discussion. Therefore, the rate of linear expansion of the sample decreased, and the densification of the sample became much more remarkable and its open porosity became remarkably less.

A higher sintering temperature led to far less porosity, and the mullitization of the composites was nearly completed at 1400 °C. Therefore, the optimum sintering temperature and soaking time were set at1400 °C and 3 h, respectively.

Table 2 lists the bulk density, open porosity, and flexural strength of the porous SiC/mullite ceramics with different graphite loadings. As the graphite loading increases, both the bulk density and flexural strength decreases, while the open porosity significantly increases. As listed in Table 2, for the bulk density, it went in the opposite way to open porosity, the flexural strength decreased from 48.14 to 18.12 MPa when the mass fraction of graphite in the SiC+Kaolin+$Al(OH)_3$ mixture increases from 0 to 0.25. As shown in Fig. 7, when the porosity increases, the flexural strength decreases exponentially. The relationship between flexural strength and open

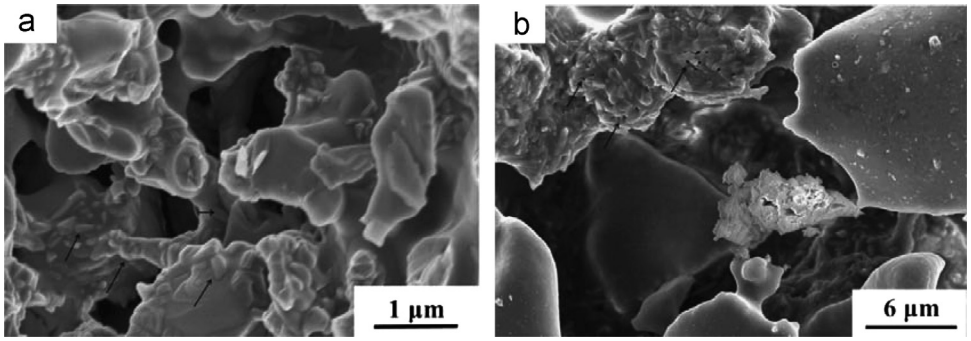

Fig. 4. Structure of the pores in the specimen sintered at 1400 °C for 3 h in air.

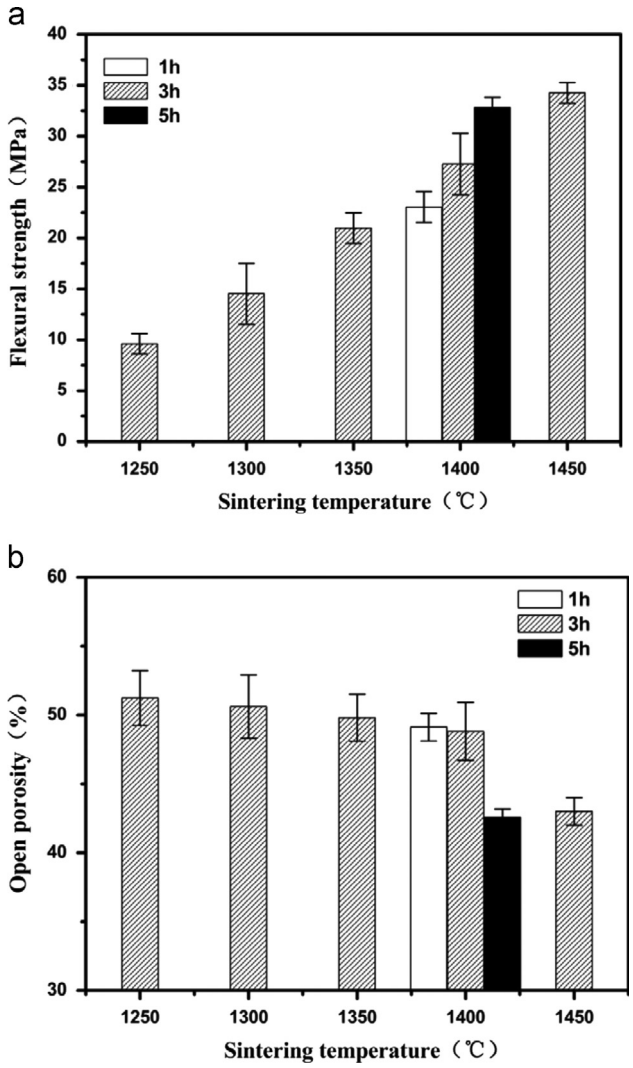

Fig. 5. Effects of sintering temperature and soaking time on (a) flexural strength and (b) open porosity of porous SiC ceramics.

porosity according to Rice is expressed as follows [27]:

$$\sigma = \sigma_0 \exp(-bp) \quad (3)$$

where σ_0 is the strength of a nonporous structure, σ the strength of the porous structure at a porosity p, and b is an empirical constant depending on the pore structure and the material composition. In this study, $\sigma_0 = 202.6$ MPa and $b = 4.26$ are obtained by fitting the experimental data with Eq. (3). Different values for b could be estimated from the strength–porosity relationship because of different oxide bond phases in oxide bonded porous SiC ceramics. She et al. obtained the value of $b = 6.5$–7.1 for SiO_2-bonded porous SiC ceramic materials with the open porosity varying between 28 and 41 vol% [11]. A lower value of $b = 4.4$ was reported by She et al. for mullite bonded porous SiC ceramics with the porosity of 28–44 vol% [10]. Therefore, the values of b would vary with processing conditions. In this study, the values of b and σ_0 appear to be quite reasonable by comparing with those reported in literature for the porous ceramics.

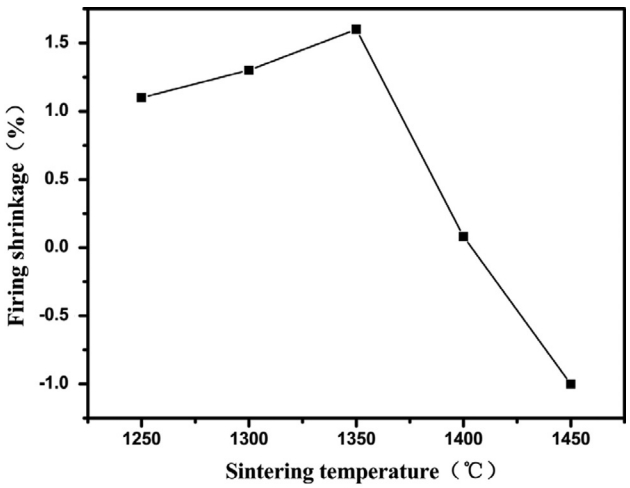

Fig. 6. Firing shrinkage of Sample 6 as functions of the sintering temperatures.

3.4. Effect of mass ratio of calcined kaolin and $Al(OH)_3$

The samples with various mass ratio of kaolin and $Al(OH)_3$ were sintered at 1400 °C for 3 h. The XRD patterns of samples are shown in Fig. 8. Mullite formation was observed in all the mixtures with different mass ratio; however, distinct mullite peaks were only observed at 40:60 mass ratio of kaolin and $Al(OH)_3$. Fig. 8d shows that not only mullite but also cristobalite and corundum co-existed in the samples. These results indicated that the phase compositions of the sintered supports could be tuned by varying the mass ratio of calcined kaolin and $Al(OH)_3$.

Table 2
Comparison of properties of sintered porous SiC ceramics with different content of graphite.

Graphite content (wt%)	Bulk density (g cm^{-3})	Open porosity (%)	Flexural strength (MPa)
0	1.52	33.98	48.14 ± 2.0
10	1.49	44.95	29.28 ± 0.8
15	1.47	48.80	27.26 ± 3.0
20	1.45	53.54	21.57 ± 1.0
25	1.42	56.03	18.12 ± 0.7

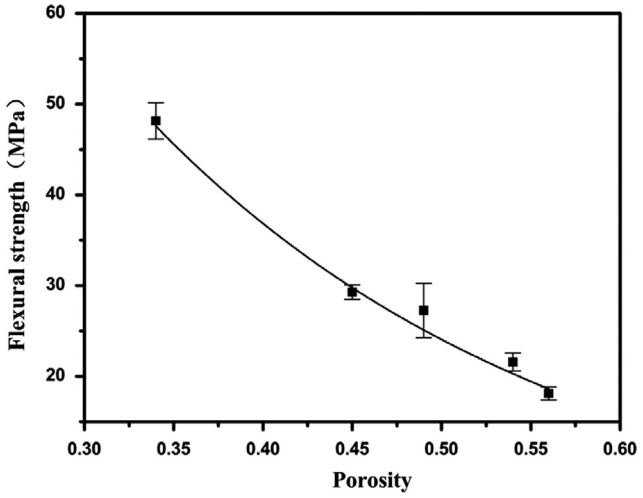

Fig. 7. Strength as a function of porosity for the porous SiC specimens, in which a 18.6 μm sized graphite powder was used as the pore former.

The open porosity and flexural strength of the porous SiC ceramics with different mass ratio of kaolin and $Al(OH)_3$ are summarized in Table 3. When the mass ratio of kaolin and $Al(OH)_3$ increases from 0.42 to 0.82, the open porosity did not change. However, the flexural strength first increases to 48.14 MPa (highest value) and then significantly decreases. This is due to the appearance of distinct Al_2O_3 peaks and the peak intensity of cristobalite has higher intensity as the content of calcined kaolin increases (Fig. 8d). According to the work by Jiahai Bai [28], more residual α-Al_2O_3 and less mullite are observed in the sample with calcined kaolin compared to the sample with uncalcined kaolin, and that the mullitization in the sample was remarkably hindered by the calcination of the kaolin. Small quantities of pores are formed by stacking residual Al_2O_3 particles which cannot touch SiC particles homogeneously and then do not completely react with SiO_2 [22]. Moreover, if SiC particles are completely oxidized to form cristobalite, a 108% volume expansion would occur. Further, excessive cristobalite is harmful to porous SiC ceramics at high temperature because its large coefficient of thermal expansion (17.5×10^{-6}/K at 293–973 K, comparing with 4.7×10^{-6}/K at 293–973 K for SiC) results in the formation of microcracks during the heating and cooling of the composites. Therefore, the open porosity increased only 3%; however, the flexural strength decreased 17.07 MPa. These results indicate that when the mass ratio of calcined kaolin and $Al(OH)_3$ is 0.67, which is slightly higher than the proportion

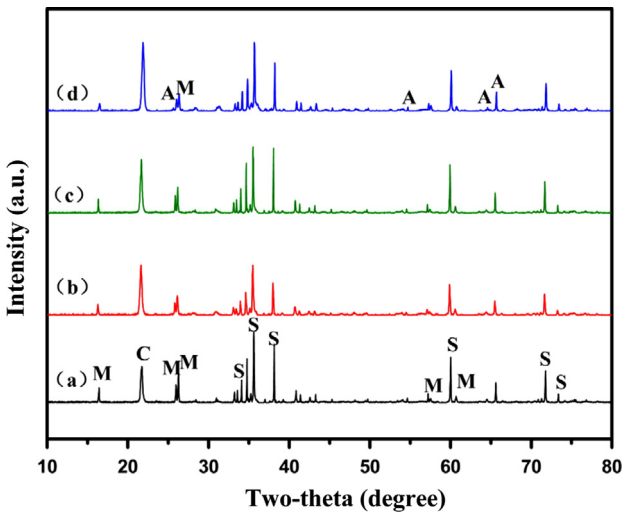

Fig. 8. XRD patterns of the specimens sintered at 1400 °C for 3 h in air with different mass ratio of kaolin and $Al(OH)_3$. (a) 30:70, (b) 35:65, (c) 40:60, and (d) 45:55 (S is SiC, M is mullite, C is cristobalite and A is Al_2O_3).

Table 3
Effects of mass ratio of calcined kaolin and $Al(OH)_3$ on open porosity and flexural strength for the porous SiC ceramics specimens at 1400 °C without the graphite.

Kaolin:$Al(OH)_3$ (wt%)	Open porosity (%)	Flexural strength (MPa)
30:70	33.96	44.34 ± 2.9
35:65	33.78	45.08 ± 2.1
40:60	33.97	48.14 ± 4.2
45:55	36.68	31.27 ± 3.4

of synthetic theory mullite, the flexural strength and open porosity of the composite in the absence of graphite were 48.14 MPa and 33.97%, respectively.

4. Conclusions

In this study, SiC/mullite composite porous ceramics were fabricated in air by a reactive processing method from calcined kaolin, $Al(OH)_3$, SiC, and graphite (as pore-forming agent). Porous SiC/mullite ceramics are bonded by the mullite and glassy phase. The results indicate that when the mass ratio of kaolin and $Al(OH)_3$ is 40:60, which is slightly higher than the theoretical mullite proportion, a flexural strength of 48.14 MPa and open porosity of 33.97% were obtained. All the samples exhibited small variations in dimension after the sintering process with a1inear expansion of 0.08–0.16%. The open porosity decreases as the sintering temperature increases; however, it increases as the graphite content increases. Further, the flexural strength of the composites was found to be inversely proportional to their open porosity. When 15% graphite was used, a flexural strength of 27.26 MPa was achieved for the composites, at an open porosity of 48.80%.

Acknowledgments

The work was supported by the 863 project under Grant no. 2012AA 03A610, Hainan University Research Fund and 211 Innovation Platform of Hainan University.

References

[1] T. Ohji, M. Fukushima, Macro-porous ceramics: processing and properties, International Materials Reviews 57 (2012) 115–131.
[2] A.R. Studart, U.T. Gonzenbach, E. Tervoort, L.J. Gauckler, Processing routes to macroporous ceramics: a review, Journal of the American Ceramic Society 89 (2006) 1771–1789.
[3] D.J. Green, P. Colombo, Cellular ceramics: intriguing structures, novel properties, and innovative applications, MRS Bulletin 28 (2003) 296–300.
[4] S. Kitaoka, Y. Matsushima, C. Chen, H. Awaji, Thermal cyclic fatigue behavior of porous ceramics for gas cleaning, Journal of the American Ceramic Society 87 (5) (2004) 906–913.
[5] J.W. Brockmayer, J.E. Dore, S. Leonard, et al., Ceramic foam filter and process for preparing same, US Patent no. 48852 63, December 5, 1989.
[6] P.C. Rojas, G.J. Piderit, P. Toro, Development of open-pore silicon carbide foams, Key Engineering Materials 132–136 (1997) 1731–1734.
[7] N. Popovska, E. Alkhateeb, A.P. Froba, A. Leipertz, Thermal conductivity of porous SiC composite ceramics derived from paper precursor, Ceramics International 36 (2010) 2203–2207.
[8] R. Riedel, G. Passing, H. Schonfelder, R.J. Brook, Synthesis of dense silicon-based ceramics at low temperatures, Nature 355 (6362) (1992) 714–717.
[9] L.S. Sigl, H.J. Kleebe, Core/rim structure of liquid-phase-sintered silicon carbide, Journal of the American Ceramic Society 76 (1993) 773–776.
[10] J. She, Z.Y. Deng, J. Daniel-Doni, T. Ohji, Oxidation bonding of porous silicon carbide ceramics, Journal of Materials Science 37 (17) (2002) 3615–3622.
[11] J. She, J.F. Yang, N. Condo, S. Kanzaki, Z.Y. Deng, High-strength porous silicon carbide ceramics by an oxidation-bonding technique, Journal of the American Ceramic Society 85 (11) (2002) 2852–2854.
[12] Y.S. Touloukian, Thermophysical Properties of Matter, IFI/Plenum Data, vol. 13, Company Press, New York, 1979.
[13] Y.F. Liu, X.Q. Liu, H. Wei, G.Y. Meng, Porous mullite ceramics from national clay produced by gel casting, Ceramics International 27 (2001) 1–7.
[14] Y.F. Chen, Y.H. Chang, M.C. Wang, M.H. Hon, Effects of Al_2O_3 addition on the phases, flow characteristics and morphology of the porous kaolin ceramics, Materials Science and Engineering A: Structural Materials Properties Microstructure and Processing 373 (2004) 221–228.
[15] S.J. Li, N. Li, Effects of composition and temperature on porosity and pore size distribution of porous ceramics prepared from $Al(OH)_3$ and kaolinite gangue, Ceramics International 33 (2007) 551–556.
[16] T. Juettner, H. Moertel, V. Svinka, R. Svinka, Structure of kaoline–alumina based foam ceramics for high temperature applications, Journal of the European Ceramic Society 27 (2007) 1435–1441.
[17] Y.F. Liu, X.Q. Liu, S.W. Tao, G.Y. Meng, O. Toff Sorensen, Kinetics of the reactive sintering of kaolinite–aluminum hydroxide extrudate, Ceramics International 28 (2002) 479–486.
[18] J. Pascual, J. Zapatero, M.C.J. de Haro, I. Varona, et al., Porous mullite and mullite-based composites by chemical processing of kaolinite and aluminum metal wastes, Journal of Materials Chemistry 10 (6) (2000) 1409–1414.
[19] G.L. Chen, H. Qi, W.H. Xing, N.P. Xu, et al., Direct preparation of macroporous mullite supports for membranes by in situ reaction sintering, Journal of Membrane Science 318 (2008) 38–44.
[20] J.H. She, Z.Y. Deng, J. Daniel-Doni, T. Ohji, Oxidation bonding of porous silicon carbide ceramics, Journal of Materials Chemistry 37 (2002) 3615–3622.
[21] K.C. Liu, G. Thomas, Time–temperature–transformation curves for kaolinite–alumina, Journal of the American Ceramic Society 77 (1994) 545–552.
[22] C.Y. Chen, G.S. Lan, W.H. Tuan, Microstructural evolution of mullite during the sintering of kaolin powder compacts, Ceramics International 26 (2000) 715–720.
[23] Y.F. Chen, M.C. Wang, M.H. Hon, Phase transformation and growth of mullite in kaolin ceramics, Journal of the European Ceramic Society 24 (2004) 2389–2397.
[24] S.Q. Ding, S.M. Zhu, Y.P. Zeng, D.L. Jiang, Fabrication of mullite-bonded porous silicon carbide ceramics by in situ reaction bonding, Journal of the European Ceramic Society 27 (4) (2007) 2095–2102.
[25] S.Q. Ding, Y.P. Zeng, D.L. Jiang, In-situ reaction bonding of porous SiC ceramics, Materials Characterization 59 (2008) 140–143.
[26] D. Das, J. Farjas, P. Roura, Passive-oxidation kinetics of SiC microparticles, Journal of the American Ceramic Society 87 (2004) 1301–1313.
[27] R.W. Rice, Comparison of stress concentration versus minimum solid area based mechanical property–porosity relations, Journal of Materials Science 28 (1993) 2187–2190.
[28] J.H. Bai, Fabrication and properties of porous mullite ceramics from calcined carbonaceous kaolin and α-Al_2O_3, Ceramics International 36 (2010) 673–678.